

# Efficient and Compact InGaAsP/Si Nanobeam Electro-optical Modulator Based on Hybrid MOS Structure

Jin Xu, An He, Xuhan Guo\* and Yikai Su

State Key Laboratory of Advanced Optical Communication Systems and Networks  
Department of Electronic Engineering, Shanghai Jiao Tong University, Shanghai, China

\*Corresponding author: [guoxuhan@sjtu.edu.cn](mailto:guoxuhan@sjtu.edu.cn)

**Abstract:** An efficient, compact photonic crystal nanobeam modulator with an InGaAsP/Si hybrid metal-oxide-semiconductor structure is proposed and simulated. The modulation efficiency is up to  $0.523 \text{ nm}/(\text{V}\cdot\mu\text{m})$  and the device length is only  $7.5 \mu\text{m}$ . © 2020 The Author(s)

## 1. Introduction

Much research has been carried out in the field of silicon (Si) photonics due to its potential applications in optical interconnects and its compatibility with the complementary metal-oxide-semiconductor (CMOS) technology. One of the workhorses for optical interconnects is the optical modulator [1] which converts electrical signals into optical signals. In particular, the modulator integrated on silicon is the key enabler for high-performance optical data communications. However, compared with materials like Lithium niobate (LN) or III-Vs, there is no significant linear electro-optical effect (mainly Pockels effect) existing in silicon because of symmetrical arrangement atoms in crystalline silicon. Hence the plasma dispersion effect (free-carrier effect) has been mainly exploited in silicon photonics for modulators.

Several types of on-chip silicon modulators have been realized by Mach-Zehnder interferometers (MZIs) [2], microring resonators (MRRs) [3], photonic crystal (PhC) nanobeam resonators [4], etc. Among these demonstrated silicon modulators, nanobeam structure has the advantage of much smaller footprint because of resonator and optical transmission waveguide seamlessly combined in one wire while still retaining a relatively high quality factor [4], which is beneficial to reducing the modulation power.

The plasma dispersion effect refers to the change of the material refractive index or absorption coefficients due to the change of free carriers concentration, and several typical schemes utilize this mechanism including: PIN injection [5], PN depletion [6] and metal-oxide-semiconductor (MOS) accumulation [7]. Among them, the MOS structure has the merits of high modulation speed and high modulation efficiency, hence more emphasis has been laid to it. However, the Si-based optical modulators suffer from low phase-modulation efficiency owing to the weak plasma dispersion effect in Si [8]. Therefore, it is essential to find a novel modulation scheme for Silicon photonics.

In this paper, electro-optical modulation in InGaAsP/Si hybrid nanobeam MOS structure based on the accumulation of electrons and holes is investigated. The InGaAsP owns a larger electron-induced refractive index change and smaller electron-induced absorption change compared with Si [8]. And the nanobeam MOS structure makes possible much smaller footprint and lower modulation power. The measured efficiency is up to  $0.523 \text{ nm}/(\text{V}\cdot\mu\text{m})$  and the length is only  $7.5 \mu\text{m}$ . This hybrid InGaAsP/Si nanobeam MOS structure provides a promising way for compact and efficient modulator.

## 2. Device design and principle

Fig. 1(a)-(c) depict the 3D, top and front views of the proposed device. It consists of hybrid InGaAsP/Si 1D PhC nanobeam waveguides and an  $\text{Al}_2\text{O}_3$  oxide layer in between. The 120-nm-thick InGaAsP layer is directly bonded above Si layer with a 5-nm-thick  $\text{Al}_2\text{O}_3$  gate oxide bonding layer. The central area of the device is the doping area, namely the modulation area. The total length ( $L_c$ ) of nanobeam cavity is only about  $7.5 \mu\text{m}$ , and the doping length ( $L_m$ ) is about  $2.5 \mu\text{m}$ . An n-type InGaAsP is employed in this structure where the refractive index can be modulated by the stronger free-carrier effect, which is critical for high-efficiency and low-loss modulation.

The resonance is created by an 1D PhC lattice with the same series of cylindrical holes in both InGaAsP and Si layers. The central nanobeam waveguide, consisting of a central-taper section and two side-reflector sections, forms a Fabry-Perot (F-P) cavity. The central-taper section with 13 holes is optimized to reduce the scattering loss and provide high phase matching between the PhC fundamental Bloch mode and the waveguide mode [9]. In the central-taper section, the radius of the hole changes from 78 nm to 61 nm, and the distance between holes changes from 284 nm to 235 nm. In the side-reflector section, the holes are evenly distributed with the radius of 78 nm and distance of 300 nm.

Fig. 1(d) shows a cross-sectional schematic and fundamental transverse electric mode of this MOS structure, in which an n-type InGaAsP layer is bonded on a p-type Si waveguide with an Al<sub>2</sub>O<sub>3</sub> layer as the bonding interface. The doping concentration in InGaAsP and Si are both  $5 \times 10^{17} \text{ cm}^{-3}$ . The fabrication of the device is expected to be the same as in [8].

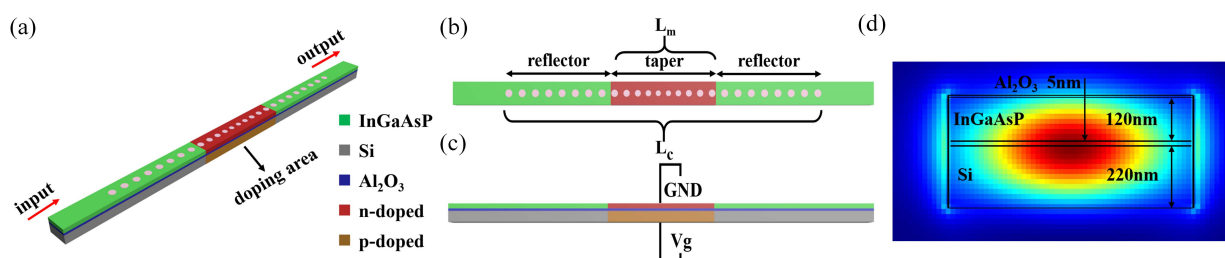


Fig. 1. Schematic configuration of the proposed InGaAsP/Si hybrid nanobeam modulator based on MOS structure; (a) The 3D view; (b) The top view; (c) The front view; (d) Central cross-sectional view of the device and its fundamental TE optical mode of InGaAsP/Si MOS structure.

The main working principle of the proposed modulator is as follows: When a positive gate voltage is applied on p-type Si, the electrons will accumulate at the upper surface of the Al<sub>2</sub>O<sub>3</sub> oxide layer and the holes accumulate at the lower surface, respectively. This redistribution of the electrons and holes causes the refractive index perturbation of a waveguide mode and thus the shift of resonant wavelength. Consequently, the electro-optical modulation is realized. With the implementation of nanobeam, the modulation efficiency and footprint can be improved.

### 3. Simulations and results

The free electrons and holes distribution applied by a bias voltage (0.6 V) are shown in Fig. 2(a)-(b) respectively, which is simulated using Finite Element Analysis. The electrons and holes will accumulate at the both sides of the oxide layer respectively when a bias voltage is applied between p-type Si and n-type InGaAsP, thereby generating the perturbation of the index. As is shown in Fig. 2(c), the changes of both free carrier concentration and the effective refractive index increase with the increasing of the bias voltage.

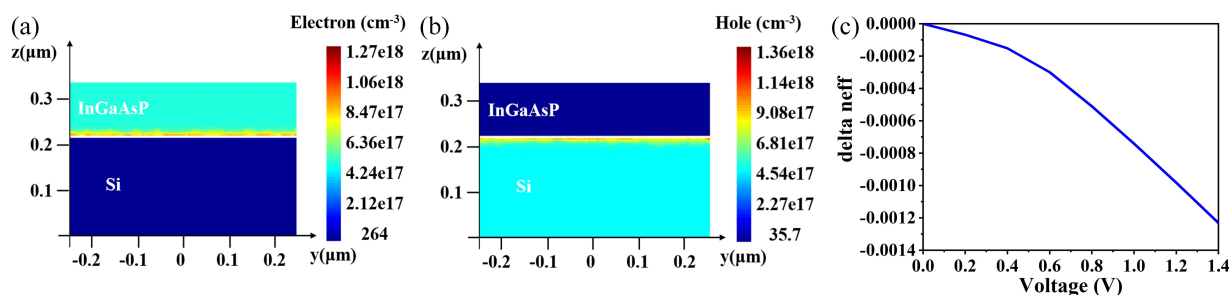


Fig. 2. (a)-(b) The free electrons and holes distribution applied by a bias voltage of 0.6V at the cross section; (c) Effective refractive index change of InGaAsP/Si hybrid nanobeam modulator at the central cross-section of the waveguide.

Fig. 3(a) shows the spectrum response at different bias voltages. It is obviously shown that the resonant wavelength was blue-shifted as the applied voltage increases. As shown in Fig. 3(b), the resonant wavelength shifts from 1560.69 nm to 1558.86 nm with the voltage increasing from 0 V to 1.4 V, which is an approximately linear relationship. Meanwhile, in Fig. 3(c), the increasing of voltage also causes the slight reduction of quality factor. From the results above, for the modulator with  $L_m = 2.5 \mu\text{m}$ , the wavelength shift in Fig. 3(b) is calculated as 1.307 nm per volt, namely  $0.523 \text{ nm}/(\text{V} \cdot \mu\text{m})$ . According to Fig. 3, efficiency can also be expressed as  $V_{\pi} * L = 1.25 \text{ V} \cdot \mu\text{m}$  (3 dB bandwidth tuning voltage multiplied by modulation length) or 1.307 nm/V (modulation length is not considered). The capacitance at 3 dB bandwidth tuning voltage is calculated as 8 fF, according to  $C = dQ/dV$ . Based on theory in [10], the energy per bit is estimated to be 0.5 fJ, which is at the reasonable level compared with similar structures in [11].

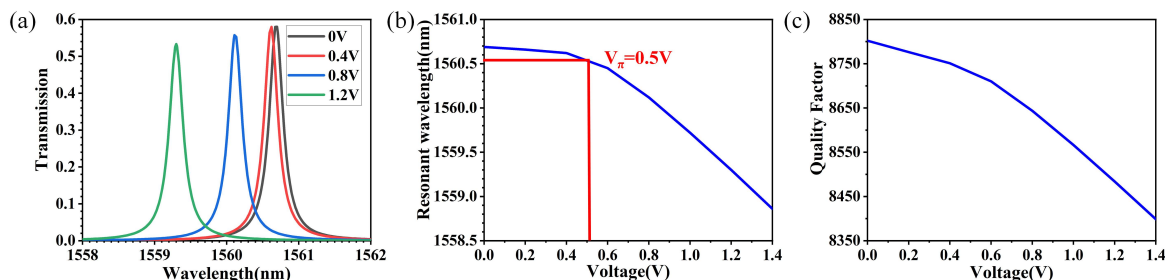


Fig. 3. (a) Spectrum response at different bias voltages; (b) Wavelength shift with voltages; (c) Quality factor change with voltages.

Table 1. Comparison of the on-chip resonator-based modulators and our devices.

Electrical Structure	Optical Structure	Efficiency <sup>(*)</sup>	Size <sup>(#)</sup>	Power consumption
MOS [12] (Expt.)	Ring	~0.0044 nm/(V* $\mu$ m)	10 $\mu$ m (R)	NA
PN [13] (Expt.)	Ring	~0.0166 nm/(V* $\mu$ m)	2.4 $\mu$ m (R)	0.9 fJ/bit
EO polymer [14] (Sim.)	Nanobeam+slot	~0.089 nm/(V* $\mu$ m)	14 $\mu$ m (L)	NA
Lateral PN [4] (Sim.)	Nanobeam	~0.13 nm/(V* $\mu$ m)	8.2 $\mu$ m (L)	14 aJ/bit
<b>This work based on hybrid MOS (Sim.)</b>	<b>Nanobeam</b>	<b>0.523 nm/(V*<math>\mu</math>m)</b>	<b>7.5 <math>\mu</math>m (L)</b>	<b>0.5 fJ/bit</b>

\* Efficiencies converted to the same unit for convenience in the table above. # R: radius; L: length.

Table 1. compares the performance of our devices with other on-chip resonator-based modulators. It is worth noting that the length of our device is 7.5  $\mu$ m and the modulation length is only 2.5  $\mu$ m, much smaller than other similar devices. It indicates that our proposed device has considerable improvement in modulation efficiency and compact size, while still retaining a relatively low power consumption.

#### 4. Conclusion

In summary, an efficient, compact photonic crystal Nanobeam modulator with an InGaAsP/Si hybrid MOS structure is demonstrated and simulated. This nanobeam modulator based on MOS structure has compact length of 7.5  $\mu$ m and high efficiency of about 0.523 nm/(V\* $\mu$ m), which is promising for low-power and high-compactness optical interconnects.

#### Funding

Open Project Program of Wuhan National Laboratory for Optoelectronics (2018WNLOKF012).

#### References

- [1] G. T. Reed, G. Mashanovich, F. Y. Gardes, and D. J. Thomson, "Silicon optical modulators," *Nature Photonics* **4**, 518-526 (2010).
- [2] M. He, M. Xu, Y. Ren, J. Jian, Z. Ruan, Y. Xu, S. Gao, S. Sun, X. Wen, L. Zhou, L. Liu, C. Guo, H. Chen, S. Yu, L. Liu, and X. Cai, "High-performance hybrid silicon and lithium niobate Mach-Zehnder modulators for 100 Gbit s<sup>-1</sup> and beyond," *Nature Photonics* **13**, 359-364 (2019).
- [3] H. Shoman, H. Jayatilaka, A. H. K. Park, A. Mistry, N. A. F. Jaeger, S. Shekhar, and L. Chrostowski, "Compact wavelength- and bandwidth-tunable microring modulator," *Opt Express* **27**, 26661-26675 (2019).
- [4] J. Hendrickson, R. Soref, J. Sweet, and W. Buchwald, "Ultrasensitive silicon photonic-crystal nanobeam electro-optical modulator: design and simulation," *Opt Express* **22**, 3271-3283 (2014).
- [5] S. Akiyama and T. Usuki, "High-speed and efficient silicon modulator based on forward-biased pin diodes," *Frontiers in Physics* **2**(2014).
- [6] J. Ding, H. Chen, L. Yang, L. Zhang, R. Ji, Y. Tian, W. Zhu, Y. Lu, P. Zhou, R. Min, and M. Yu, "Ultra-low-power carrier-depletion Mach-Zehnder silicon optical modulator," *Opt Express* **20**, 7081-7087 (2012).
- [7] J. K. Park, S. Takagi, and M. Takenaka, "InGaAsP Mach-Zehnder interferometer optical modulator monolithically integrated with InGaAs driver MOSFET on a III-V CMOS photonics platform," *Opt Express* **26**, 4842-4852 (2018).
- [8] J.-H. Han, F. Boeuf, J. Fujikata, S. Takahashi, S. Takagi, and M. Takenaka, "Efficient low-loss InGaAsP/Si hybrid MOS optical modulator," *Nature Photonics* **11**, 486-490 (2017).
- [9] H. Y. Zhou, C. Y. Qiu, X. H. Jiang, Q. M. Zhu, Y. He, Y. Zhang, Y. K. Su, and R. Soref, "Compact, submilliwatt, 2 x 2 silicon thermo-optic switch based on photonic crystal nanobeam cavities," *Photon. Res.* **5**, 108-112 (2017).
- [10] D. A. Miller, "Energy consumption in optical modulators for interconnects," *Opt Express* **20 Suppl 2**, A293-308 (2012).
- [11] E. Li and A. X. Wang, "Theoretical Analysis of Energy Efficiency and Bandwidth Limit of Silicon Photonic Modulators," *Journal of Lightwave Technology* **37**, 5801-5813 (2019).
- [12] X. Huang, D. Liang, C. Zhang, G. Kurczveil, and R. Beausoleil, "Heterogeneous MOS microring resonators," in 2017 IEEE Photonics Conference (IPC), 2017,
- [13] E. Timurdogan, C. M. Sorace-Agaskar, J. Sun, E. Shah Hosseini, A. Biberian, and M. R. Watts, "An ultralow power athermal silicon modulator," *Nat Commun* **5**, 4008 (2014).
- [14] B. Qi, P. Yu, Y. B. Li, X. Q. Jiang, M. Yang, and J. Y. Yang, "Analysis of Electrooptic Modulator With 1-D Slotted Photonic Crystal Nanobeam Cavity," *Ieee Photonics Technology Letters* **23**, 992-994 (2011).